Journal of Molecular Structure 1225 (2021) 129149

Contents lists available at ScienceDirect

Journal of Molecular Structure

journal homepage: www.elsevier.com/locate/molstr

Synthesis, characterization and cytotoxic activity evaluation of 4-(1,2,3-triazol-1-yl) salicylic acid derivatives

Zita G. Ríos-Malváez[a,b], Ma-Angeles Cano-Herrera[a,b], Juan Carlos Dávila-Becerril[a], Gustavo Mondragón-Solórzano[a], María Teresa Ramírez-Apan[c], David Morales-Morales[c], Joaquín Barroso-Flores[a,c], Jonnathan G. Santillán-Benítez[b], M.V. Basavanag Unnamatla[a,b], Marco Antonio García-Eleno[a,b], Nelly González-Rivas[a,b], Erick Cuevas-Yañez[a,b,*]

[a] Centro Conjunto de Investigación en Química Sustentable UAEM-UNAM. Carretera Toluca-Atlacomulco Km 14.5, Universidad Autónoma del Estado de México, Toluca, Estado de México, 50200, México
[b] Facultad de Química, Universidad Autónoma del Estado de México. Paseo Colón esq. Paseo Tollocan, 50120, Toluca, Mexico
[c] Instituto de Química, Universidad Nacional Autónoma de México, Circuito Exterior S. N., Ciudad Universitaria, Coyoacán, Ciudad de México, 04510, Mexico

ARTICLE INFO

Article history:
Received 10 May 2020
Revised 7 August 2020
Accepted 26 August 2020
Available online 26 August 2020

Keywords:
1,2,3-Triazoles
anticancer
click chemistry
salicylic acid derivatives

ABSTRACT

A novel series of 4-(1,2,3-triazol-1-yl) salicylic acid derivatives was synthesized from 4-azidosalicylic acid and diverse alkynes using copper catalyzed azide-alkyne cycloaddition as key process and fully characterized by using different analytical techniques. The *in vitro* antiproliferative activity of these new compounds was explored against a series of tumoral cell lines which included U251 (human glioblastoma), PC-3 (human prostate cancer cell line), K562 (human leukemia), HCT-15 (human colorectal adenocarcinoma), MCF-7 (human breast adenocarcinoma) and SKLU (human lung adenocarcinoma), showing selective activity in some compounds. Moreover, molecular docking studies suggest a strong interaction between ARG-154 in STAT3 and the triazole fragment which can explain the inhibitory activity observed in these compounds.

1. Introduction

Nowadays cancer represents one of the most challenging diseases in the world. In this regard, the signal transducer and activator of transcription 3 (STAT3) is a cytosolic protein identified as a key regulator of human cancers that contributes to uncontrolled differentiation, proliferation, survival and tumorigenesis. Recent studies have shown that STAT3 factor is active in many types of cancer including breast, stomach, brain and lung [1]. STAT3 belongs to a family of transcription factors (TFs) of STAT type (signal transducer and activator of transcription) which play an important role in cell growth described in the activation of about 70% of both solid and hematological tumors [2]. Hence, some current therapies aimed to treat various types of cancer are based on the inhibition of the STAT3 factor using diverse compounds such as N-[2-(1,3,4-oxadiazolyl)]-4-quinolinecarboxamide derivatives [3], anthraquinone compounds [4,5], bis-dipicolylamine copper(II) complexes [6], and 4-aminosalicylic acid derivatives (molecule **1**, scheme 1) that have demonstrated antiproliferative activity by inhibition of the STAT3 phosphorylation process inducing apoptosis in cell lines at low concentrations [7–9].

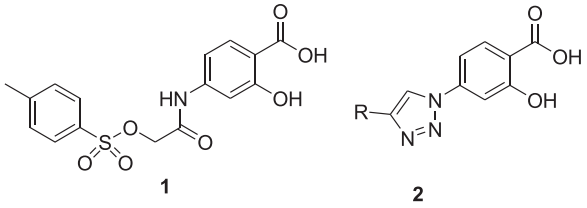

Scheme 1. Structure of 4-aminosalicylic acid derivatives **1** and general structure for molecules **2** proposed in this work.

These elements prompted us to investigate the possible application of CuAAC reaction, the best-known click reaction, in the preparation of a series of 4-aminosalicylic acid derivatives. Because 1,2,3-triazoles derived from CuAAC reaction are amide bioisosteres and biocompatible molecular structures for drug design [10–13], we proposed the synthesis of triazolyl salicylic acid derivatives **2** as 4-aminosalicylic acid derivatives aimed to find more and better STAT3 inhibitors. Herein is described a summary of our recent successful endeavors in this area.

* Corresponding author.
E-mail address: ecuevasy@uaemex.mx (E. Cuevas-Yañez).

https://doi.org/10.1016/j.molstruc.2020.129149
0022-2860/

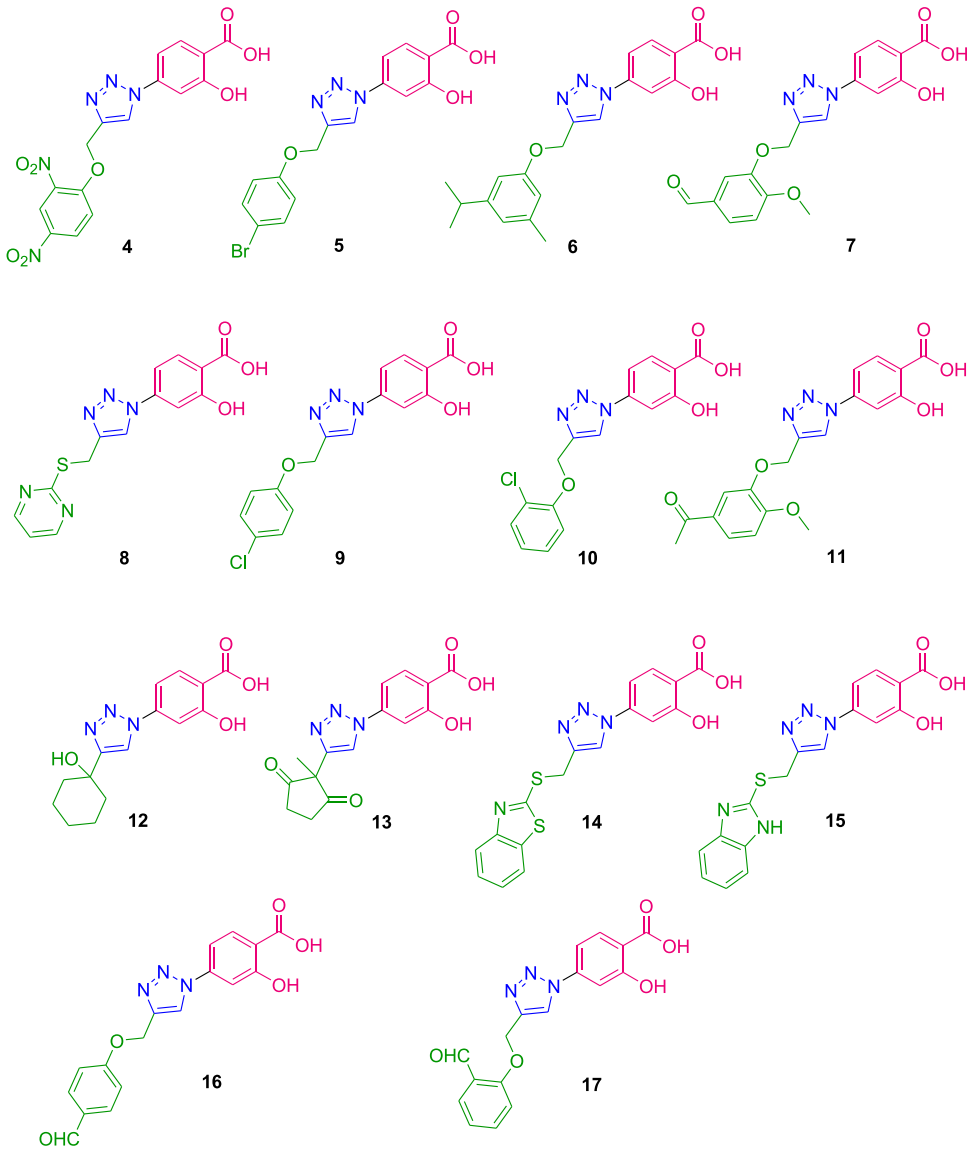

Scheme 2. Structure of 4-(1,2,3-triazol-1-yl) salicylic acid derivatives **4**-**17**.

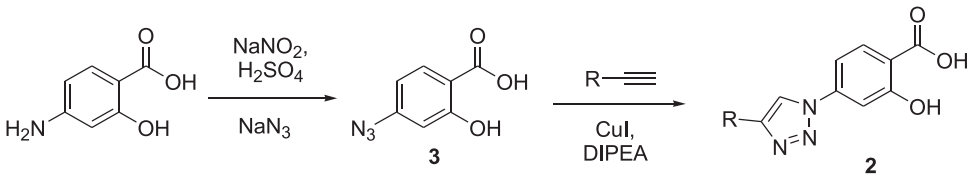

Scheme 3. Synthesis of 4-(1,2,3-triazol-1-yl) salicylic acid derivatives.

2. Experimental

2.1. General Remarks

The starting materials were purchased from Aldrich Chemical Co. and were used without further purification. Solvents were distilled before use. Silica plates of 0.20 mm thickness were used for thin layer chromatography. Melting points were determined with a Krüss Optronic melting point apparatus and they are uncorrected. ^{1}H and ^{13}C NMR spectra were recorded using a Bruker Avance 300 MHz, and a Varian 500 MHz; the chemical shifts (δ) are given in ppm relative to TMS as internal standard (0.00). For analytical purposes the mass spectra were recorded on a Shimadzu GCMS-QP2010 Plus in the EI mode, 70 eV, 200°C via direct inlet probe. Only the molecular and parent ions (m/z) are reported. IR spectra were recorded on a Bruker TENSOR 27 FT instrument.

2.2. Synthesis of 4-Azido-2-hydroxybenzoic acid (**3**)

Typical procedure. A solution of $NaNO_2$ (1.3 g, 18.84 mmol) in H_2O (12.5 mL) was added to a cold solution of 4-amino-2-hydroxybenzoic acid (2.06 g, 13.46 mmol) and H_2SO_4 (5mL) in H_2O (30 mL) and the resulting mixture was stirred at 0°C for 20 min. Urea (7 g) was added keeping the temperature at 0°C and a solution of NaN_3 (2 g, 30.7 mmol) in H_2O (10 mL) was added. The product was filtered under reduced pressure and washed with

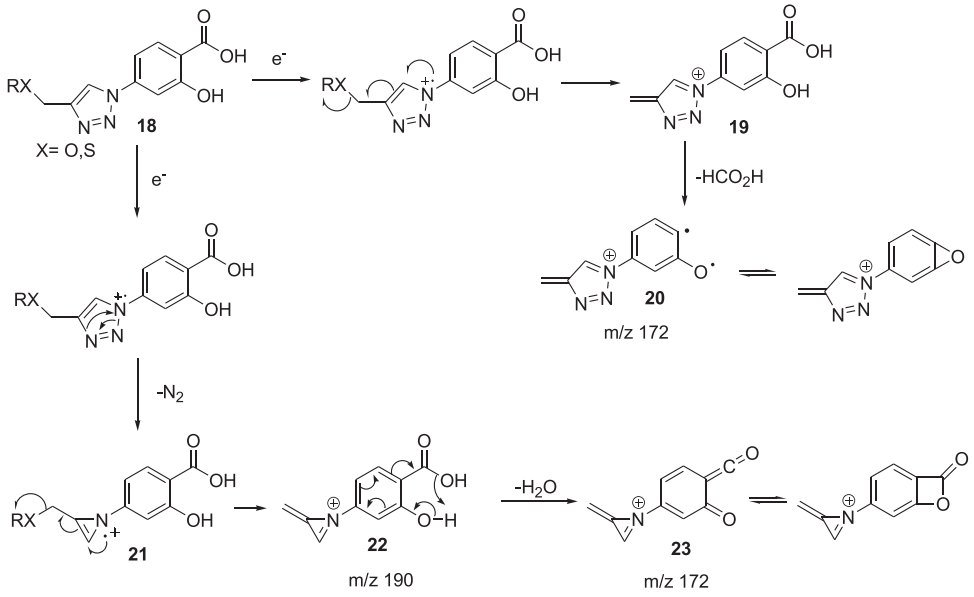

Scheme 4. Fragmentation mechanisms for 4-(1,2,3-triazol-1-yl) salicylic acid derivatives.

cold H_2O (30 mL). Purification by crystallization (EtOH) afforded 4-Azido-2-hydroxybenzoic acid **3** as pale-yellow solid (2.07 g, 11.5 mmol, 86 %), m. p. 160°C (lit. 160-161°C) [14]. UV (MeOH) λ_{max} (log ε) 272 (1.197), 310 (0.589) nm. IR (ATR) ν_{max} 3600, 3200, 2104, 1757 cm^{-1}. ^1H NMR: (300 MHz, $CDCl_3$) δ = 8.91 (s, 1H), 8.49 (s, 1H), 7.59 – 7.22 (m, 2H). ^{13}C NMR: (75 MHz, $CDCl_3$) δ = 170.75 (C), 169.34 (C), 145.43 (C), 124.93 (CH), 112.42 (CH), 108.02 (C), 107.35 (CH).

2.3. General procedure of synthesis of 4-(1,2,3-triazol-1-yl) salicylic acid derivatives

A solution of the corresponding alkyne (1.0 mmol) in CH_2Cl_2 (0.5 mL) was added to a solution of 4-azido-2-hydroxybenzoic acid **3** (11.43 mmol), CuI (0.010 g, 0.052 mmol) and DIPEA (0.5 mL) in CH_2Cl_2 (1.5 mL). The mixture was stirred at room temperature for 24 h. The solvent was removed under reduced pressure, a 0.2 % aqueous solution of EDTA (5 mL) was added and the mixture was stirred at room temperature for 30 min. A 1 M HCl solution was added (2 mL) and the product was filtered and washed with H_2O (5 mL). The product was purified by crystallization (MeOH). Compounds **4**-**17** are represented in Scheme 2.

*4-(4-((2,4-dinitrophenoxy)methyl)-1,2,3-triazol-1-yl)-2-hydroxy-benzoic acid (**4**)*

4-azido-2-hydroxybenzoic acid **3** and 2,4-dinitro-1-prop-2-ynyloxy-benzene afforded 4-(4-((2,4-dinitrophenoxy)methyl)-1,2,3-triazol-1-yl)-2-hydroxybenzoic acid as a white solid. Yield: 0.127g (34 %), m. p. 200°C. UV (MeOH) λ_{max} (log ε) 256 (0.090) nm. IR (ATR) ν_{max} 3200, 2900, 1700, 1640, 1600, 1520, 1480, 1300 cm^{-1}. ^1H NMR: (300 MHz, DMSO-d_6) δ 14.84 (s, 1H), 11.54 (s, 1H), 8.74 (t, J = 3.0 Hz, 1H), 8.49 (dd, J = 9.1, 3.0 Hz, 1H), 8.41 (s, 1H), 8.04 (s, 1H), 7.74 (d, J = 9.2 Hz, 1H), 7.53 (d, J = 3.2 Hz, 1H), 7.27 (s, 1H), 7.19 (s, 1H), 5.61 (s, 2H). ^{13}C NMR: (75 MHz, DMSO-d_6) δ = 155.36 (C), 139.74 (C), 138.41 (2XC), 128.66 (2xCH), 121.84 (CH), 121.11 (2xCH), 115.22 (CH), 108.47 (CH), 107.42 (C), 63.30 (CH_2). MS [EI+] m/z (%): 401 $[M]^+$ (5), 172 $[M\text{-}C_{10}H_9N_3O_3]^+$ (100). Anal. calcd. for $C_{16}H_{11}N_5O_8$ (%): C 47.89, H 2.76, N 17.45; found: C 47.85, H 2.77, N 17.41.

*4-[4-(4-Bromophenoxymethyl)-1,2,3-triazol-1-yl]-2-hydroxy-benzoic acid (**5**)*

4-azido-2-hydroxybenzoic acid **3** and 1-Bromo-4-prop-2-ynyloxy-benzene afforded 4-[4-(4-Bromophenoxymethyl)-1,2,3-triazol-1-yl]-2-hydroxy-benzoic acid as a white solid. Yield: 0.298 g (73 %), m.p. 190°C. UV (MeOH) λ_{max} (log ε) 255 (0.101) nm. IR (ATR) ν_{max} 3180, 3100, 1680, 1600, 1450, 1287, 820, 790, 700 cm^{-1}. ^1H NMR: (300 MHz, DMSO-d_6) δ 8.96 (s, 1H), 8.49 (s, 1H), 7.86 (d, J = 8.1 Hz, 1H), 7.55 – 7.41 (m, 2H), 7.25 (d, J = 8.8 Hz, 2H), 7.10 – 7.03 (m, 2H), 5.22 (s, 2H). ^{13}C NMR: (75 MHz, DMSO-d6) δ = 170.55 (C), 163.94 (C), 157.25 (2xC), 143.47 (C), 139.44 (C), 132.19 (2xCH), 131.49 (CH), 122.93 (C), 117.11 (2xCH), 112.42 (CH), 107.97 (CH), 107.35 (CH), 61.20 (CH_2). MS [EI+] m/z (%): 189 $[M]^+$ (12), 190 $[M\text{-}C_{10}H_5N_3O]^+$ (89), 172 $[M\text{-}C_9H9NO_3]^+$ (100), 114 $[M\text{-}C_{13}H_{13}\ N_3O_4]^+$ (40). Anal. calcd. for $C_{16}H_{12}BrN_3O_4$ (%): C 49.25, H 3.10, N 10.77; found: C 49.29, H 3.07, N 10.71.

*2-Hydroxy-4-[4-(3-isopropyl-5-methyl-phenoxymethyl)-1,2,3-triazol-1-yl]-benzoic acid (**6**)*

4-azido-2-hydroxybenzoic acid **3** and 1-isopropyl-3-methyl-5-prop-2-ynyloxy-benzene afforded 2-hydroxy-4-[4-(3-isopropyl-5-methyl-phenoxymethyl)-1,2,3-triazol-1-yl]-benzoic acid as a white solid. Yield: 0. 189 g (43 %), m.p. 202°C. UV (MeOH) λ_{max} (log ε) 257 (0.315), 313 (0.133) nm. IR (ATR) ν_{max} 3600, 3200, 1680, 1600, 1450, 1290 cm^{-1}. ^1H NMR: (300 MHz, DMSO-d_6) δ 8.87 (s, 1H), 7.99 (d, J = 8.5 Hz, 1H), 7.59 – 7.36 (m, 2H), 6.86 – 6.50 (m, 3H), 5.19 (s, 2H), 2.83 (p, J = 6.9 Hz, 1H), 1.21 (d, J = 6.9 Hz, 6H). ^{13}C NMR: (75 MHz, DMSO-d_6) δ = 171.25 (C), 162.42 (C), 157.93 (C), 149.81 (C), 144.25 (C), 140.95 (C), 131.87 (CH), 122.25 (CH), 119.79 (CH), 113.50 (CH), 112.24 (CH), 109.86 (CH), 109.75 (CH), 107.52 (CH), 60.77 (CH_2), 33.43 (CH_3), 23.66 (CH_3), 21.20 (CH_3). MS [EI+] m/z (%): 367 $[M]^+$ (21), 190 $[M\text{-}C_{12}H_{17}O]^+$ (65), 172 $[M\text{-}C_8H_9N_3O_3]^+$ (75), 150 $[M\text{-}C_{10}H_7O_3N_3]^+$ (96), 135 $[M\text{-}C_{13}H_{18}ON_3]^+$ (100), 119 $[M\text{-}C_5H_{11}O_3]^+$ (40), 91 $[M\text{-}C_{14}H_{16}N_2O_4]^+$ (75). Anal. calcd. for $C_{20}H_{21}N_3O_4$ (%): C 65.38, H 5.76, N 11.44; found: C 65.45, H 5.71, N 11.41.

*4-[4-(4-Formyl-2-methoxy-phenoxymethyl)-1,2,3-triazol-1-yl]-2-hydroxy-benzoic acid (**7**)*

4-azido-2-hydroxybenzoic acid **3** and 3-methoxy-4-prop-2-ynyloxy-benzaldehyde afforded 4-[4-(4-formyl-2-methoxy-phenoxymethyl)-1,2,3-triazol-1-yl]-2-hydroxy-benzoic acid as a

pale-yellow solid. Yield: 0.298 g (84 %), m.p. 185°C. UV (MeOH) λ_{max} (log ε) 273 (0.0451), 312 (0.037) nm. IR (ATR) ν_{max} 3500, 3200, 1680, 1640, 1470, 1265 cm^{-1}. ^1H NMR: (300 MHz, DMSO-d_6) δ 9.79 (s, 1H), 8.88 (s, 1H), 7.75 (d, J = 8.1 Hz, 1H), 7.52 (dd, J = 8.3, 1.9 Hz, 1H), 7.37 (d, J = 8.4 Hz, 1H), 7.35 (d, J = 1.8 Hz, 1H), 7.13 – 7.01 (m, 2H), 5.26 (s, 2H), 3.75 (s, 3H). ^{13}C NMR: (75 MHz, DMSO-d_6) δ = 191.50 (C), 170.44 (C), 164.72 (C), 152.76 (C), 149.33(C), 142.86 (C), 138.73(C), 131.21 (CH), 130.02 (CH), 125.93 (CH), 123.31 (CH), 120.31 (CH), 112.68 (C), 109.71 (C), 107.26 (CH), 107.04 (CH), 61.58 (CH_2), 55.51 (CH_3). MS [EI+] m/z (%): 369[M]$^+$ (5), 310 [M-$C_2H_3O_2$] $^+$ (10), 190 [M-C_9H9NO_3] $^+$ (61), 172 [M-C_8H_{11} N_3O_3] $^+$ (72), 151 [M-$C_{10}H_8$ N_3O_3] $^+$ (100), 133 [M-$C_{12}H_{16}$ N_2O_3] $^+$ (59), 105 [M-$C_{13}H_{16}$ N_2O_4] $^+$ (72). Anal. calcd. for $C_{18}H_{15}N_35O_6$ (%): C 58.54, H 4.09, N 11.38; found: C 58.57, H 4.07, N 11.35.

*2-Hydroxy-4-[4-(pyrimidin-2-ylsulfanylmethyl)-1,2,3-triazol-1-yl]-benzoic acid (**8**)*

4-azido-2-hydroxybenzoic acid **3** and 2-prop-2-ynylsulfanyl-pyrimidine afforded 2-hydroxy-4-[4-(pyrimidin-2-ylsulfanylmethyl)-1,2,3-triazol-1-yl]-benzoic acid as a pale-yellow solid. Yield: 0.078 g (64 %), m.p. 205°C. UV (MeOH) λ_{max} (log ε) 274 (0.400), 311 (0.338) nm. IR (ATR) ν_{max} 3150, 3060, 1660, 1610, 1560, 1450, 1380, 1300 cm^{-1}. ^1H NMR: (300 MHz, DMSO-d_6) δ 8.76 (s, 1H), 8.62 (d, J = 4.9 Hz, 2H), 7.86 (s, 1H), 7.46 (s, 1H), 7.40 (s, 1H), 7.19 (t, J = 4.9 Hz, 1H), 4.46 (s, 2H). ^{13}C NMR: (75 MHz, DMSO-d6) δ = 169.93 (2xC), 157.94 (2xCH), 144.98 (C), 140.94 (C), 132.41 (CH), 121.71 (CH), 117.50 (2xCH), 110.00 (CH), 107.81 (C), 53.55 (CH_2). MS [EI+] m/z (%): 329[M] $^+$ (30), 227 [M-$C_3H_6N_2S$] $^+$ (30), 172 [M-$C_4H_7N_5S$] $^+$ (100), 119 [M-C_9H_{12} N_3OS] $^+$ (60). Anal. calcd. for $C_{14}H_{11}N_5O_3S$ (%): C 51.06, H 3.37, N 21.27; found: C 51.09, H 3.39, N 21.28.

*4-[4-(4-Chloro-phenoxymethyl)-1,2,3-triazol-1-yl]-2-hydroxy-benzoic acid (**9**)*

4-azido-2-hydroxybenzoic acid **3** and 1-chloro-4-prop-2-ynyloxy-benzene afforded 4-[4-(4-chloro-phenoxymethyl)-1,2,3-triazol-1-yl]-2-hydroxy-benzoic acid as a pale-yellow solid. Yield: 0.309 g (89 %), m.p. 199-200°C. UV (MeOH) λ_{max} (log ε) 273 (0.053), 312 (0.045) nm. IR (ATR) ν_{max} 3550, 3200,1680, 1600, 1480, 1310 cm^{-1}. ^1H NMR: (300 MHz, DMSO-d_6) δ 9.08 (s, 1H), 7.96 (s, 1H), 7.63 (s, 1H), 7.54 (s, 1H), 7.41–7.32 (m, 2H), 7.16 – 7.07 (m, 2H), 5.25 (s, 2H). ^{13}C NMR: (75 MHz, DMSO-d_6) δ = 156.71 (C), 143.84 (C), 141.09 (C), 129.26 (2xCH), 129.18 (C), 124.69 (CH), 123.04 (CH), 116.61 (C), 116.52 (2xCH), 110.36 (CH), 108.12 (C), 61.19 (CH_2). MS [EI+] m/z (%): 345 [M]$^+$ (14), 190 [M-$C_7H_3N_3O$]$^+$ (81), 172 [M-C_9H9NO_3]$^+$ (100), 128 [M-$C_{11}H_{11}N_3O_2$]$^+$ (49). Anal. calcd. for $C_{16}H_{12}ClN_3O_4$ (%): C 55.58, H 3.50, N 12.15; found: C 55.51, H 3.54, N 12.17.

*4-[4-(2-Chloro-phenoxymethyl)-1,2,3-triazol-1-yl]-2-hydroxy-benzoic acid (**10**)*

4-azido-2-hydroxybenzoic acid **3** and 1-chloro-2-prop-2-ynyloxy-benzene afforded 4-[4-(2-chloro-phenoxymethyl)-1,2,3-triazol-1-yl]-2-hydroxy-benzoic acid as a white solid. Yield: 0.247 g (68 %), m.p. 200-201°C. UV (MeOH) λ_{max} (log ε) 273 (0.052), 311 (0.044) nm. IR (ATR) ν_{max} 3200, 2800, 1680, 1600, 1440, 1295 cm^{-1}. ^1H NMR: (300 MHz, DMSO-d_6) δ 9.03 (s, 1H), 7.92 (d, J = 8.3 Hz, 1H), 7.52 – 7.45 (m, 2H), 7.41 – 7.22 (m, 4H), 6.94 (dd, J = 7.4, 1.6 Hz, 1H), 5.27 (s, 2H). ^{13}C NMR: (75 MHz, DMSO-d_6) δ = 171.04 (C), 162.42 (C), 152.51 (C), 146.44 (C), 141.09 (CH), 130.08 (CH), 128.33 (CH), 128.15 (C), 123.26 (CH), 122.21 (CH), 122.03 (CH), 121.49 (C), 107.77 (CH), 106.83 (C), 61.77 (CH_2). MS [EI+] m/z (%): 345 [M]$^+$ (9), 190 [M-$C_7H_3N_3O$]$^+$ (65), 172 [M-C_9H9NO_3]$^+$ (100), 128 [M-$C_{11}H_{11}N_3O_2$]$^+$ (50). Anal. calcd. for $C_{16}H_{12}ClN_3O_4$ (%): C 55.58, H 3.50, N 12.15; found: C 55.59, H 3.56, N 12.13.

*4-[4-(4-Acetyl-2-methoxy-phenoxymethyl)-1,2,3-triazol-1-yl]-2-hydroxy-benzoic acid (**11**)*

4-azido-2-hydroxybenzoic acid **3** and 1-(3-methoxy-4-prop-2-ynyloxy-phenyl)ethanone afforded 4-[4-(4-Acetyl-2-methoxy-phenoxymethyl)-1,2,3-triazol-1-yl]-2-hydroxy-benzoic acid as a pale yellow solid. Yield: 0.140 g 81 %), m.p. 210°C. UV (MeOH) λ_{max} (log ε) 270 (0.226), 307 (0.154) nm. IR (ATR) ν_{max} 3200, 1680, 1590, 1490, 1270 cm^{-1}. ^1H NMR: (300 MHz, DMSO-d_6) δ 9.07 (s, 1H), 7.97 (d, J = 8.2 Hz, 1H), 7.65 (dd, J = 8.4, 2.0 Hz, 1H), 7.55 – 7.41 (m, 3H), 7.32 (d, J = 8.4 Hz, 1H), 5.33 (s, 2H). ^{13}C NMR: (75 MHz, DMSO-d_6) δ = 196.39 (C), 171.55 (C), 170.94 (C), 162.50 (C), 151.54 (C), 148.73 (C), 143.44 (C), 140.68 (C), 132.06 (CH), 130.37 (CH), 123.36 (CH), 122.89 (CH), 112.38 (CH), 110.44 (CH), 109.80 (C), 107.67 (CH), 61.44 (CH_2), 55.46 (CH_3), 26.34 (CH_3). MS [EI+] m/z (%): 383[M]$^+$ (5), 204 [M-$C_9H_{13}N_3O$]$^+$ (90), 165 [M-$C_{12}H_{16}N_3O$]$^+$ (100), 114 [M-$C_{16}H_{19}N_3O$]$^+$ (75). Anal. calcd. for $C_{19}H_{17}N_3O_6$ (%): C 59.53, H 4.47, N 10.96; found: C 59.55, H 4.43, N 10.98.

*2-Hydroxy-4-[4-(1-hydroxycyclohexyl)-1,2,3-triazol-1-yl]-benzoic acid (**12**)*

4-azido-2-hydroxybenzoic acid **3** and 1-ethynylcyclohexanol afforded 2-hydroxy-4-[4-(1-hydroxycyclohexyl)-1,2,3-triazol-1-yl]-benzoic acid as a pale-yellow solid. Yield: 0.267 g (88 %), m.p. 225°C UV (MeOH) λ_{max} (log ε) 235 (0.198), 257 (0.461) nm. IR (ATR) ν_{max} 3250, 3140, 2900, 2800, 1650, 1620, 1440, 1300 cm^{-1}. ^1H NMR: (300 MHz, DMSO-d_6) δ 8.67 (s, 1H), 7.93 – 7.85 (m, 1H), 7.51 – 7.42 (m, 2H), 1.88 (ddd, J = 13.8, 10.4, 3.8 Hz, 2H), 1.76 – 1.59 (m, 4H), 1.44 – 1.31 (m, 3H), 1.23 – 1.17 (m, 1H). ^{13}C NMR: (75 MHz, DMSO-d_6) δ = 171.13 (C), 162.21(C), 156.92 (C), 141.45 (C), 132.14 (CH), 119.50 (CH), 113.06 (C), 109.99 (CH), 107.29 (CH), 67.89 (CH_2), 37.56 (2xCH_2), 25.21 (CH_2), 21.68 (2xCH_2). MS [EI+] m/z (%): 303 [M]$^+$ (5), 190 [M-$C_5H_{11}N$]$^+$ (60), 172 [M-$C_8H_7N_2$]$^+$ (55), 114 [M-$C_{10}H_{11}N_3O$]$^+$ (100),

72 [M-$C_{14}H_{21}N_3$]$^+$ (90). Anal. calcd. for $C_{15}H_{17}N_3O_4$ (%): C 59.40, H 5.65, N 13.85; found: C 59.43, H 5.67, N 17.87.

*2-Hydroxy-4-[4-(1-methyl-2,5-dioxo-cyclopentylmethyl)-1,2,3-triazol-1-yl]-benzoic acid (**13**)*

4-azido-2-hydroxybenzoic acid **3** and 2-methyl-2-prop-2-ynyl-cyclopentane-1,3-dione afforded 2-hydroxy-4-[4-(1-methyl-2,5-dioxo-cyclopentylmethyl)-1,2,3-triazol-1-yl]-benzoic acid as a pale yellow solid. Yield: 0.136 g (41 %), m.p. 185°C. UV (MeOH) λ_{max} (log ε) 256 (0.0239), 270 (0.201) nm. IR (ATR) ν_{max} 3110, 1680, 1605, 1440, 1400, 1305, 1200cm^{-1}. ^1H NMR: (300 MHz, DMSO-d_6) δ 8.55 (s, 1H), 7.89 (d, J = 8.4 Hz, 1H), 7.29 (d, J = 7.7 Hz, 3H), 3.03 (s, 2H), 2.89 – 2.67 (m, 4H), 1.14 (s, 4H). ^{13}C NMR: (75 MHz, DMSO-d_6) δ = 216.10 (2xC), 171.89 (2xC), 163.05(C), 143.40 (C), 140.23 (C), 131.90 (CH), 120.85 (CH), 108.99 (CH), 107.37 (CH), 54.86 (C), 54.66 (2xCH_2), 34.77 (CH_2), 20.27 (CH_3). MS [EI+] m/z (%): 329 [M]$^+$ (15), 190 [M-$C_7H_9NO_2$]$^+$ (53), 172 [M-$C_8H_{15}NO_2$]$^+$ (70), 42 [M-$C_{16}H_{21}N_3O_2$]$^+$ (100). Anal. calcd. for $C_{16}H_{15}N_3O_5$ (%): C 58.36, H 4.59, N 12.76; found: C 58.38, H 4.61, N 12.74.

*4-[4-(Benzothiazol-2-ylsulfanylmethyl)-1,2,3-triazol-1-yl]-2-hydroxy-benzoic acid (**14**)*

4-azido-2-hydroxybenzoic acid **3** and 2-prop-2-ynylsulfanyl-benzothiazole afforded 4-[4-(Benzothiazol-2-ylsulfanylmethyl)-1,2,3-triazol-1-yl]-2-hydroxy-benzoic acid as a white solid. Yield: 0.169 g (42 %), m.p. 205°C. UV (MeOH) λ_{max} (log ε) 281 (0.032) nm. IR (ATR) ν_{max} 3560, 2990, 1680, 1460, 1380, 1330, 1230 cm^{-1}. ^1H NMR: (300 MHz, DMSO-d_6) δ 8.80 (s, 1H), 7.99 (d, J = 8.1 Hz, 1H), 7.90 (t, J = 9.1 Hz, 2H), 7.47 (t, J = 7.6 Hz, 1H), 7.36 (t, J = 7.3 Hz, 1H), 7.26 (d, J = 8.1 Hz, 2H), 4.76 (s, 2H). ^{13}C NMR: (75 MHz, DMSO-d_6) δ = 171.57 (C), 165.69 (2xC), 152.71 (C), 140.0 (C), 134.87 (C), 131.92 (C), 126.62 (C), 126.55 (CH), 124.73

(2xCH), 121.91 (2xCH), 121.43 (2xCH), 108.76 (CH), 107.52 (CH), 51.22 (CH_2). MS [EI+] m/z (%): 384[M]$^+$ (5), 248 [M-$C_7H_{10}N_3$]$^+$ (30), 166 [M-$C_{10}H_{10}N_3O_3$]$^+$ (50), 69 [M-$C_{15}H_{16}N_4S_2$]$^+$ (100), 55 [M-$C_{16}H_{26}N_4S_2$]$^+$ (90). Anal. calcd. for $C_{17}H_{12}N_4O_3S_2$ (%): C 53.11, H 3.15, N 14.57; found: C 53.18, H 3.17, N 14.54.

*4-[4-(1H-Benzoimidazol-2-ylsulfanylmethyl)-1,2,3-triazol-1-yl]-2-hydroxy-benzoic acid (**15**)*

4-azido-2-hydroxybenzoic acid **3** and 2-prop-2-ynylsulfanyl-1H-benzoimidazole afforded 4-[4-(1H-benzoimidazol-2-ylsulfanylmethyl)-1,2,3-triazol-1-yl]-2-hydroxy-benzoic acid as a white solid. Yield: 0.228 g (62 %), m.p. 220°C. UV (MeOH) λ_{max} (log ε) 256 (0.218) nm. IR (ATR) ν_{max} 3026, 1670, 1610, 1560, 1450, 1290, 1230 cm^{-1}. ^{1}H NMR: (300 MHz, DMSO-d_6) δ 8.92 (s, 1H), 8.82 (s, 1H), 7.91 (d, J = 8.4 Hz, 2H), 7.64 (ddd, J = 8.8, 6.0, 2.8 Hz, 2H), 7.41 (d, J = 7.3 Hz, 3H), 7.24 – 7.18 (m, 2H), 5.54 (s, 2H). ^{13}C NMR: (75 MHz, DMSO-d_6) δ = 171.47 (C), 171.00 (C), 150.38 (C), 143.34 (C), 142.97 (C), 140.71 (C), 140.59 (C), 132.05 (2xCH), 122.07 (CH), 121.95 (CH), 117.93 (CH), 110.17 (C), 109.76 (CH), 107.60 (CH), 107.55 (CH), 54.56 (CH_2). MS [EI+] m/z (%): 367 [M]$^+$ (40), 210 [M-$C_5H_9N_4S$]$^+$ (20), 188 [M-$C_7H_5N_3O_3$]$^+$ (35),172 [M-$C_9H_{13}N_3S$]$^+$ (50), 146 [M-$C_{10}H_{13}N_4S$]$^+$ (100), 88 [M-$C_{14}H_{15}N_5S$]$^+$ (40). Anal. calcd. for $C_{17}H_{13}N_5O_3S$ (%): C 55.58, H 3.57, N 19.06; found: C 55.55, H 3.59, N 19.11.

*4-[4-(4-Formylphenoxymethyl)-1,2,3-triazol-1-yl]-2-hydroxy-benzoic acid (**16**)*

4-azido-2-hydroxybenzoic acid **3** and 4-prop-2-ynyloxy-benzaldehyde afforded 4-[4-(4-formylphenoxymethyl)-1,2,3-triazol-1-yl]-2-hydroxy-benzoic acid as a white solid. Yield: 0.290 g (85 %), m.p. 210°C. UV (MeOH) λ_{max} (log ε) 273 (0.208) nm. IR (ATR) ν_{max} 3100, 1690, 1600, 1500, 1480, 1300, 1250 cm^{-1}. ^{1}H NMR: (300 MHz, DMSO-d_6) δ 9.89 (s, 1H), 9.06 (s, 1H), 8.00 (d, J = 8.3 Hz, 1H), 7.90 (d, J = 7.9 Hz, 2H), 7.53 (s, 1H), 7.26 (dd, J = 8.9, 5.5 Hz, 2H), 5.38 (s, 2H). ^{13}C NMR: (75 MHz, DMSO-d_6) δ = 191.09 (C), 171.27 (C), 162.26(C), 162.23 (C), 143.53 (C), 141.25 (C), 132.21 (CH), 131.83 (2xCH), 130.01 (C), 123.09 (CH), 115.20 (2xCH), 113.05 (CH), 110.36 (C), 107.79 (CH), 61.32 (CH_2). MS [EI+] m/z (%): 339 [M]$^+$ (15), 190 [M-$C_7H_7N_3O$]$^+$ (85), 172 [M-$C_8H_{13}N_3O$]$^+$ (100). Anal. calcd. for $C_{17}H_{13}N_3O_5$ (%): C 60.18, H 3.86, N 12.38; found: C 60.19, H 3.88, N 12.36.

*4-[4-(2-Formylphenoxymethyl)-1,2,3-triazol-1-yl]-2-hydroxy-benzoic acid (**17**)*

4-azido-2-hydroxybenzoic acid **3** and 2-prop-2-ynyloxy-benzaldehyde afforded 4-[4-(2-Formylphenoxymethyl)-1,2,3-triazol-1-yl]-2-hydroxy-benzoic acid as a white solid. Yield: 0.252g (78 %), 220°C. UV (MeOH) λ_{max} (log ε) 273 (0.324) nm. IR (ATR) ν_{max} 3440, 1685, 1675, 1600, 1485, 1280, 1200 cm^{-1}. ^{1}H NMR: (300 MHz, DMSO-d_6) δ 10.38 (s, 1H), 9.06 (s, 1H), 7.91 (d, J = 8.4 Hz, 1H), 7.64 (dd, J = 11.6, 7.6 Hz, 2H), 7.54 – 7.35 (m, 3H), 7.06 (t, J = 7.5 Hz, 1H), 5.39 (s, 2H). ^{13}C NMR: (75 MHz, DMSO-d_6) δ = 189.44 (C), 170.99 (C), 162.28 (C), 160.27 (C), 143.91 (C), 140.92 (C), 136.37 (CH), 132.12 (CH), 127.62 (CH), 124.57 (C), 122.78 (C), 121.29 (CH), 114.15 (CH), 110.07 (CH), 107.69 (CH), 106.77 (C), 62.17 (CH_2). MS [EI+] m/z (%): 401 [M]$^+$ (5), 172 [M-C10H9N3O3]$^+$ (100). Anal. calcd. for $C_{17}H_{13}N_3O_5$ (%): C 60.18, H 3.86, N 12.38; found: C 60.15, H 3.84, N 12.39.

2.4. Cell lines culture and culture medium

The compounds were screened *in vitro* against human cancer cell lines: HCT-15 (human colorectal adenocarcinoma), MCF-7 (human mammary adenocarcinoma), K562 (human chronic myelogenous leukemia), U251 (human glioblastoma), PC-3 (human prostatic adenocarcinoma) which were supplied by National Cancer Institute (USA); SKLU-1 (human lung adenocarcinoma) from National Institute of Cancerology, Mexico, and COS-7, adherent monkey kidney fibroblasts (ATTC).

The human tumor cytotoxicity was determined using the protein-binding dye sulforhodamine B (SRB) in microculture assay to measure cell growth, as described in the protocols established by the NCI [15]. The cell lines were cultured in RPMI-1640 medium supplemented with 10% fetal bovine serum, 2mM L-glutamine, Penicillin-Streptomycin solution 100x (Gibco) and 1% non-essential amino acids (Gibco®). They were maintained at 37°C in humidified atmosphere with 5% CO_2. The viability of the cells used in the experiments exceed 95% as determined with trypan blue.

2.5. Cytotoxicity assay

Cytotoxicity after treatment of the tumors cells and normal cell with the test compounds was determined using the protein-binding dye sulforhodamine B (SRB) in microculture assay to measure cell growth as described in the reference [15]. The cells were removed from the tissue culture flasks by treatment with trypsin and diluted with fresh media. Of this cell suspension, 100 μl containing 5000-10,000 cell per well, were pipetted into 96 well microtiter plates (Costar) and the material was incubated at 37°C for 24 h in a 5% CO_2 atmosphere. Each cell line is deposited by triplicate and subsequently, 100 μl of a solution of the compound obtained by diluting the stocks were added to each well. The cultures were exposed for 48 h to the compound at concentrations 25 µM. After the incubation period, cells were fixed to the plastic substratum by the addition of 50 μl of cold 50 % aqueous trichloroacetic acid. The plates were incubated at 4°C for 1 h, washed with tap H_2O, and air-dried. The trichloroacetic-acid-fixed cells were stained by the addition of 0.4% SRB. Free SRB solution was the removed by washing with 1% aqueous acetic acid. The plates were the air-dried, and the bound dye was solubilized by the addition of 10 mM unbuffered Tris base (100 μl). The plates were placed on a shaker for 10 min, and the absorption was determined at 515 nm using an ELISA plate reader (Bio-Tex Instruments).

2.6. Molecular modeling

All optimizations of compounds **4**-**17** were performed at ωB97X-D/6-311+G(d,p) level of theory. Frequencies were calculated to confirm that the structures are on an energetic minimum. For docking calculations, the PDB files of STAT 3 protein (1BHH for SH2 domain and 4ZIA for N-terminal domain) were used from Protein Data Bank. The best binding modes were chosen by binding energy and the type of interactions between the aminoacids and the compounds **4-17**. These binding sites were isolated and partially optimized, leaving backbone atoms fixed and sidechains flexibles. Also, hydrogens on backbone atoms were optimized. A first pre-optimization with PM6 semiempirical method was performed and a ωB97X-D/cc-pVDZ level of theory partial optimization were performed later. Non-Covalent Interactions index (NCI) was performed on these sites for a complete study of the intermolecular interactions on binding sites. Geometry optimizations with quantum mechanics methods were performed with Gaussian09 Rev. E.01 package [16], and docking calculations were performed with AutoDockTools 1.5.6 version package [17]. NCI análisis were performed with a DensToolkit development version [18].

3. Results and discussion

3.1. Chemistry

Initial studies were focused to prepare 4-azido-2-hydroxybenzoic acid **3** from a modification of the procedure

Table 1
Synthesis of 4-(1,2,3-triazol-1-yl) salicylic acid derivatives.

Compound	R^1	% Yield
4	$CH_2O(2,4\text{-}NO_2)C_6H_3$	85
5	$CH_2O(4\text{-}Br)C_6H_4$	99
6	$CH_2O(3\text{-}iPr\text{-}5\text{-}CH_3)C_6H_3$	43
7	$CH_2O(2\text{-}OCH_3\text{-}4\text{-}CHO)C_6H_3$	84
8	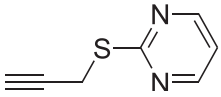	64
9	$CH_2O(4\text{-}Cl)C_6H_4$	89
10	$CH_2O(2\text{-}Cl)C_6H_4$	68
11	$CH_2O(2\text{-}OCH_3\text{-}4\text{-}COCH_3)C_6H_3$	46
12	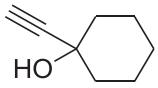	51
13	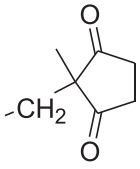	66
14	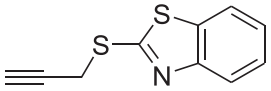	84
15	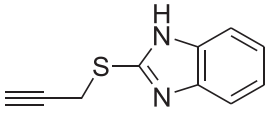	55
16	$CH_2O(4\text{-}CHO)C_6H_4$	66
17	$CH_2O(2\text{-}CHO)C_6H_4$	68

described by Dupuis [14] through a consecutive diazotization-azidation process on 4-amino-2-hydroxybenzoic acid (Scheme 3). A characteristic band at 2104 cm^{-1} corresponding to stretching N=N=N azide vibration [19] is present in the IR spectrum; furthermore, carboxylic acid group was identified by the C=O stretching vibration band at 1757 cm^{-1} and a wide O-H stretching band at 3600 cm^{-1}; an additional O-H vibration band (3200 cm^{-1}) corroborates salicylic acid arrange in agreement to previous reports [20–22] which also describe a strong absorption peak found approximately at 270 nm in the respective UV spectra.

Subsequent CuAAC reaction of azide **3** with the appropriate alkynes in presence of catalytic amounts of CuI afforded the corresponding 4-(1,2,3-triazol-1-yl) salicylic acid derivatives **4**-**17** in 43-99% yields. The results in Table 1 illustrate the product yields and the functional groups used on the alkyne part which integrate the substituents at C5 position in obtained triazole rings.

Compounds **4**-**17** are quite stable in solution after 48 h, which is important to know because these molecules are structural specifics and there are not transformations in solution. The 1,2,3-triazole moiety in these compounds was unambiguously determined by the conventional spectroscopic techniques; for instance, IR spectra of triazoles **4**-**17** exhibit the distinctive aromatic C=C stretching vibration band at 1600 cm^{-1} together to a N=N band at 1450 cm^{-1} according to literature [23–26]. A remarkable absorption band detected in these spectra is located at 1300 cm^{-1} which has been correlated to a cyclic -N-N=N- configuration present in 1,2,3-triazole core [27,28]. On the other hand, high energy absorption bands ranged at 255-280 nm are present in UV spectra of compounds **4**-**17** which are assigned to a $\pi \rightarrow \pi^*$ transition in aromatic rings [29].

The presence of 1,2,3-triazole ring was categorically established through the NMR spectra analysis. In this way, a typical singlet signal assigned to the hydrogen on triazole C-5 at 7.5-8.8 ppm is observed in ^{1}H NMR spectra of compounds **4**-**17**, whereas the corresponding ^{13}C NMR spectra reveal C-4 and C-5 triazole carbon signals at 143 and 112 ppm respectively. Some selected spectral data of compounds triazoles **4**-**17** are summarized in Table 2.

A noteworthy fact derived from MS analysis that should be considered to complete this spectroscopic information is the appearance in most of mass spectra of specific ions at m/z 190 and at m/z 172 which in some cases is presented as base peak. Two possible fragmentation patterns to rationalize these peaks are showed in Scheme 4. An ionization on triazole N1 followed by loss of RO·/RS· fragment generates a methylene triazolium ion **19** which in turn loses HCO_2H to give radical cation **20** with m/z 172. Other plausible fragmentation mechanism involves the well documented extrusion of N_2 from 1,2,3-triazole [30,31] affording azirinyl radical cation **21** which undergoes a cleavage of RO-CH_2/RS-CH_2 bond providing successively methylene azirinyl cations **22** (m/z 190) and **23** (m/z 172) after losing of H_2O.

3.2. Biological evaluation and Cytotoxic Activity

The anti-proliferative activity of compounds **4**–**17** was evaluated against a series of tumoral cell lines which included U251 (human glioblastoma), PC-3 (human prostate cancer cell line), K562 (human leukemia), HCT-15 (human colorectal adenocarcinoma), MCF-7 (human breast adenocarcinoma) and SKLU (human lung adenocarcinoma), the results are summarized in Table 3.

Although a direct comparison among all these compounds is not simple, some relationships can be found through an analysis of compounds that share common structural features. Thus, in order to facilitate this analysis, four groups of 4-(1,2,3-triazol-1-yl) salicylic acid derivatives were considered according to a structural similarity premise.

A first 4-(1,2,3-triazol-1-yl) salicylic acid group included phenoxymethyl derivatives substituted at C4 position on triazole moiety (compounds **4-7, 9-11, 16** and **17**). In general, these molecules exhibit good activities for HCT-15, U251 and MCF-7, however, these compounds are also toxic against COS7 healthy cells. The molecule that displays the highest toxicity in this group is compound **6**, with 64.64% cell growth inhibition against HCT-15 and 52.3 % inhibition against COS7 cell lines. This activity can be attributed to the bioavailability provided by the *m*-cymene moiety present in several natural products with well-known biological activity [32,33]. Other interesting example from this triazole group is compound **4** bearing a 2,4-dinitrophenyl fragment which probably causes the high activity against HCT-15 (39.0 % cell growth inhibition) and also against COS7 (30.6 %) due to the nitro group ability to interact with biological nucleophiles such as proteins, amino acids, nucleic acids, and enzymes through non-covalent interactions found in some antineoplasic, antibiotic, and antiparasitic agents which contain this group [34]. On the other hand, the aryl methoxy group together with aldehyde/ketone carbonyl group present in molecules **11** and **7** promotes a low polarity effect and formation of non-covalent hydrogen interactions with carbonyl substituent increasing the cytotoxic activity observed in these compounds, 45.2% growth inhibition against PC-3 cells with compound **7**, whereas compound **11** showed 32.85% growth inhibition against MCF-7 cells.

An outstanding characteristic perceived in a second 4-(1,2,3-triazol-1-yl) salicylic acid derivatives group is the existence of an alicyclic part directly attached to the triazole ring bearing a cyclohexanol fragment in compound **12** or a methylcyclopentanedione moiety in compound **13**, which resulted more active in this series with 52.4% and 38.05% growth inhibition of U251 and HCT-15 cell lines respectively, but also more toxic against healthy cells (47.4% cell growth inhibition of COS7). This behavior could be related to the chemical nature of the cyclopentanedione fragment present in several biologically active natural products [35,36] as well as other

Table 2
Selected spectral data of 4-(1,2,3-triazol-1-yl) salicylic acid derivatives.

Compound	λ_{max}	log ε	IR (ν_{max}, cm^{-1})			^{1}H NMR (ppm)	^{13}C NMR (ppm)	
			C=C$_{arom}$	N=N$_{arom}$	-N-N=N-	Triazole C5-H	C4	C5
4	256	0.090	1600	1480	1300	8.04	139.7	115.2
5	255	0.101	1600	1450	1287	8.49	143.4	112.4
6	257	0.315	1600	1450	1290	7.99	144.5	112.2
7	273	0.045	1640	1470	1265	8.88	142.8	112.6
8	274	0.400	1610	1450	1300	7.86	144.9	110.0
9	273	0.053	1600	1480	1310	7.54	143.8	110.3
10	273	0.052	1600	1440	1295	7.52	146.4	107.7
11	270	0.226	1590	1490	1270	7.55	143.4	112.3
12	257	0.461	1620	1440	1300	7.93	141.4	109.9
13	256	0.023	1605	1440	1305	7.89	143.4	108.9
	270	0.201						
14	281	0.032	1680	1460	1330	7.99	140.0	108.7
15	256	0.218	1610	1450	1290	7.91	143.3	110.1
16	273	0.208	1600	1480	1300	7.53	143.5	110.3
17	273	0.324	1600	1485	1280	7.54	143.9	110.0

Table 3
Growth inhibition (%) of tumor cell lines at 25 μM by compounds **4**-**17**[a]

Compound	U251	PC-3	K562	HCT-15	MCF-7	SKLU-1	COS7
4	18.28	NC[b]	9.0	39.03	20.6	NC	30.61
5	12.0	9.9	18.1	26.53	17.3	NC	16.9
6	23.43	NC	13.56	64.64	10.5	NC	52.3
7	4.4	45.2	9.4	26.56	NC	NC	20.3
8	20.45	3.9	15.23	67.63	20.41	NC	44.28
9	2.5	9.1	12.7	16.3	11.8	NC	2.5
10	NC	NC	4.2	19.1	3.5	NC	5.0
11	10.66	NC	10.21	10.57	32.85	NC	9.13
12	11.01	NC	3.6	17.21	23.23	NC	5.26
13	52.4	NC	13.9	38.05	11.69	NC	47.4
14	11.55	NC	4.86	10.93	33.53	NC	14.67
15	57.9	NC	5.51	35.24	NC	NC	47.64
16	4.66	NC	NC	6.25	12.82	NC	3.96
17	6.78	NC	1.28	8.97	20.41	NC	8.71

[a] The values indicate the mean calculated from experiments conducted in triplicate.
[b] NC: not cytotoxic.

similar nitrogen 5-membered rings such as pyrrole and phthalimide analogs used as anticancer agents [37]. Moreover, this observed activity can also be boosted by the potential ability of compound **13** to promote non-covalent interactions in physiologic media due to the presence of the two bioavailable ketone groups. These compounds are interesting; however, their toxicity against healthy cells reduces their potential attractiveness for further studies.

Group 3 of 4-(1,2,3-triazol-1-yl) salicylic acid derivatives comprises heterocyclic rings attached to 1,2,3-triazole moiety through a -SCH2- linkage, these heterocycles include pyrimidine in compound **8**, benzothiazole (**14**) and benzimidazole (**15**) which would incorporate the well-known biological activities from these heterocyclic fragments to final molecules. The results of cytotoxic activity show that compounds **8** and **15** are highly active against HCT-15 (67.63 and 35.24 % respectively) but at the same time these molecules display high toxicity to COS7 cells (44.28 and 47.64 % respectively) as well as other groups discussed above. A noteworthy property found in compound **14** is the selective activity against MCF-7 cell line (33.53 % cell growth inhibition) in contrast to activity against HTC-15 and COS7 (10.93 and 14.67% cell growth inhibition respectively). On the other hand, triazole **15** proved to be the most active compound of this series, showing 57.9 % growth inhibition of U251 cells, 35.24 % growth inhibition of HCT-15 and 47.64 % growth inhibition of COS7 cells. This feature could drive next investigations to study the effect of substituents in benzimidazole core on antitumoral activity of this kind of molecules.

A fourth group of triazoles involves compounds **5, 9, 10, 16** and **17** holding halogen atoms and aldehyde/ketone carbonyl groups in their structures. From this group, benzaldehyde derivatives revealed activity against MCF-7, 20.41 and 12.82% cell growth inhibition respectively for **17** and **16** besides low toxicity against COS7 cells (8.71 and 3.96 % cell growth inhibition for compounds **17** and **16** respectively). In this case, the aldehyde substituent clearly plays a relevant role in the triazole activity which is almost duplicated by changing the position in the aromatic ring from 4- to 2-, this behavior is also reflected in the toxicity of these compounds against healthy cells. The cytotoxic activity of this pair of compounds contrasts to observed activity in compounds **5, 9** and **10** which produce 26.53, 16.3 and 19.1 % growth inhibition into HCT-15 cells similar to aldehyde derivatives discussed above and considerably less active than triazoles classified in other series. However, a promising molecule in this group is triazole **10** which exhibits 19.1 % cell growth inhibition against HCT-15 cancer cells and low toxicity with healthy COS7 cells (5.0 %). In addition, this compound is quite selective showing no activity against U251, PC-3 and SKLU-1 cancer cell lines, and just a reduced toxicity with K562 (4.2 %) and MCF-7 (3.5 %) cancer cells, which is apparently associated with *o*- position between substituents in aromatic ring identified in other molecules with this substitution pattern and similar activity. Although this work is not conclusive, it provides several lines that should be explored, some of which are currently under development in our research group.

Inhibitory activity showed by compounds **4-17** is comparable to some 1,2,3-triazole-based tumor cell growth inhibitors [38–45]. This feature opens the possibility of considering 4-(1,2,3-triazol-1-yl) salicylic acid derivatives as an emerging group of STAT3 in-

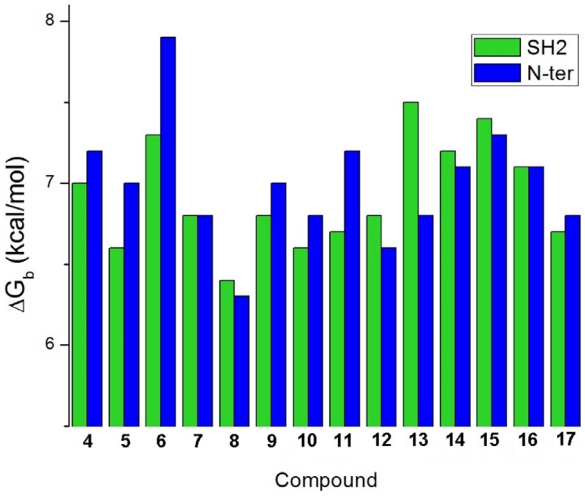

Fig. 1. Docking interaction energies by domain.

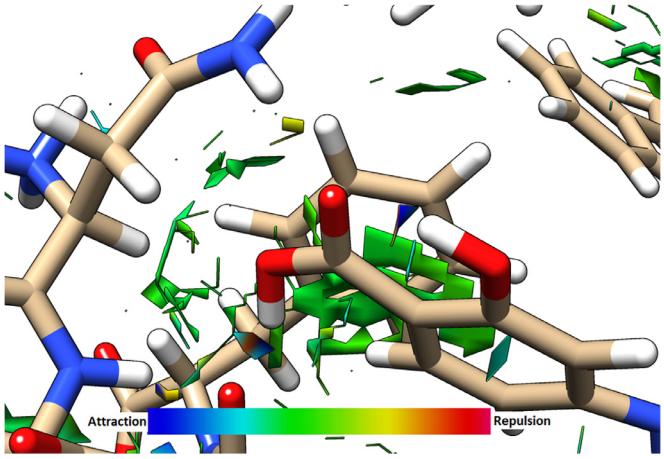

Fig. 2. Intermolecular interactions between **6** and SH2.

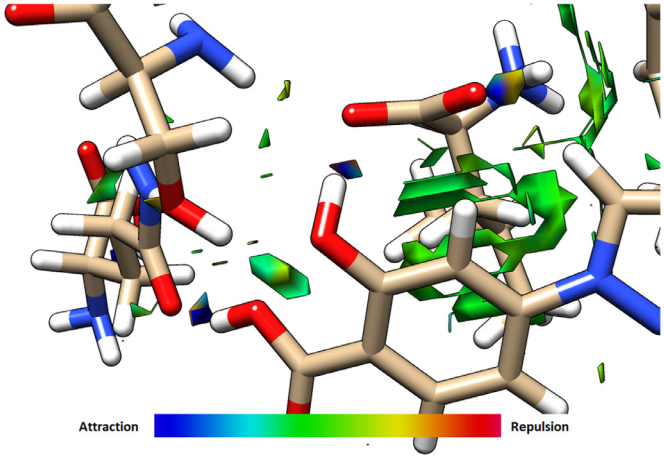

Fig. 3. Non-covalent interactions between **6** and predicted N-Terminal binding site. The H-bonds between the carboxylate of the salicylate group and the amino acids are shown in blue.

hibitors together to other small molecules [46–49]. Accordingly, further studies will be necessary to modify biological activity providing higher selectivity in terms of a cytotoxic activity increase against specific cancer lines with low impact to healthy cells including intensive studies on antiproliferative activity against tumor renewal [50]. These challenges might be overcome through the use of the Click Chemistry approach due to this concept would allow an easy biological activity modulation by a simple functional group exchange in alkyne fragment; these are some advantages of using 1,2,3-triazole moiety as a versatile scaffold, besides possessing a metal coordination ability which gives an additional chance to extend inhibitory potency such as Kandioller and coworkers have observed [51].

3.3. Molecular modeling

All optimized geometries show an intramolecular H-bond in the salicylate fragment. The structures are enough rigid by not showing any additional intramolecular interactions. STAT3 protein is one of the most studied cancer-related factors, being modeled by classical molecular dynamics and molecular docking [52] and also docking calculations for inhibit the STAT3 dimerization [53], however, there was none work with triazole-derivatives as a STAT3 inhibitors.

A blind molecular docking was carried out into both SH2 and N-terminal domains. Most of the molecules show a high affinity to N-terminal domain, such as the delta G binding energy is in the range from 6.3 to 7.9 kcal/mol, but for the SH2 domain the delta G binding energy range is from 6.4 to 7.5 kcal/mol (Fig. 1). By comparing binding energies, only four compounds show more affinity for the SH2 domain, and two show the same binding energy for the SH2 and N-terminal domains, which means that compounds are non-selective through the STAT3 principal domains.

The best binding models were chosen from each domain, two for SH2 domain and three for N-Terminal domain. In both domains are shown hydrogen bonds between the amino acids in the binding site and the compounds synthesized in this work. For SH2 domain, compounds **4** and **6** represent the best binding models, whereas for the N-Terminal domain, **6, 12** and **13** are the best binding models.

For SH2 domain, compound **6** shows hydrogen bonds, also π-stacking between the salicylate ring and the PHE-191 residue (Fig. 2). The carboxylate group from salicylate ring is H-bond acceptor and donor with the surrounding amino acids, such as ASN-185 and the GLY-190 residues.

Other representative intermolecular interaction displayed with SH2 domain involves H-bonds between the SER-158-backbone residue and R fragment as well as steric interactions with SER-164 residue. In addition, an interaction with the triazole fragment and ARG-154 residue is also detected.

For N-Terminal domain, all models include H-bonds between salicylate fragment and amino acids, like in SH2 model, with GLN-3 and with SER-113. The compound that showed the best affinity by energy binding with N-terminal domain is **6** (Fig. 3), but the protein-ligand interactions shown on docking are only two H-bonds: one between the salicylate and the GLN-3, the salicylate and LEU-109 and a Van Der Waals interaction between the triazole and ALA-44. This means that the H-bonds are quite strong to bind the ligand consistent with experimental inhibition results and the Van Der Waals interaction is not affecting the binding mode by a repulsive interaction one.

Steric interactions are also important between **4** and N-Terminal binding site. As shown in Fig. 3, the salicylate ring interacts with the LEU-109 sidechain. On the studied models there are strong H-bonds between the salicylate group and the amino acid sidechains (Fig.s 4 and 5).

H-bond interactions between salicylate fragment and amino acids in both domains are constant and consistent in all binding sites given by the blind docking, but also π-stacking interactions are present on many of the chosen models. These interactions are quite strong to explain experimental biological activity. Therefore,

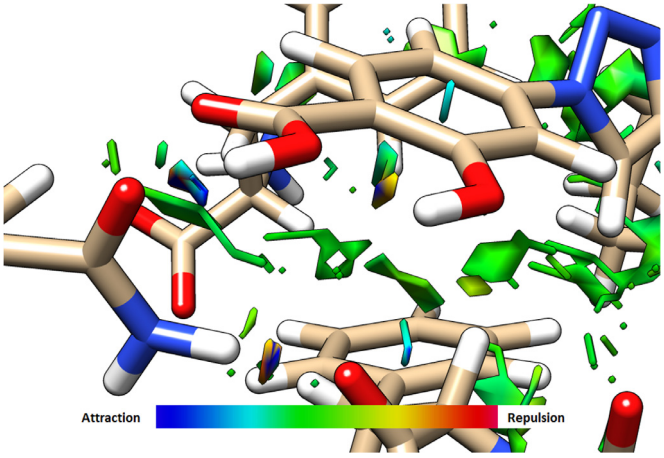

Fig. 4. Intermolecular interactions between **12** and N-Terminal domain. H-bond interactions are shown in blue.

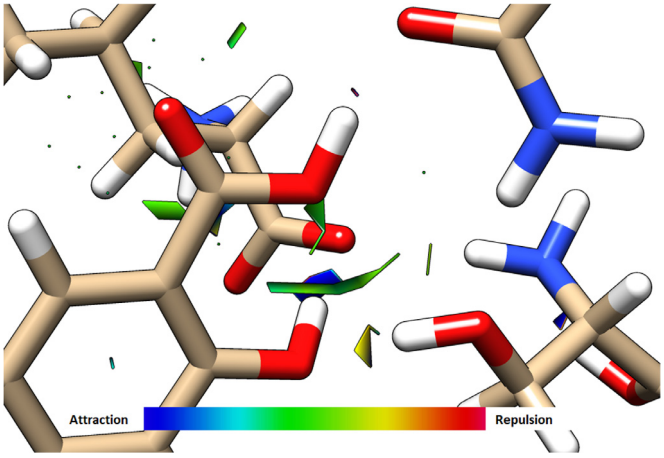

Fig. 5. Non-covalent interactions between **13** and N-Terminal domain. The H-bonds are shown in blue.

molecular docking calculations suggest a non-selective binding site between domains due to the similar binding energies in both SH2 and N-terminal domains.

As far we know, these are the first examples of 1,2,3-triazolyl compounds derived from 4-amino salicylic acid displaying anticancer activity and providing new opportunities to design and synthesize more STAT 3 inhibitors, either as antitumor agents themselves or as a part of a combined therapy [54].

4. Conclusions

In brief, CuAAC reaction demonstrated to be a useful method in the preparation of a collection of 4-(1,2,3-triazol-1-yl) salicylic acid derivatives with outstanding specific activity against some tumoral cell lines. According to experimental data, the theoretical results show that the interactions are crucial into the molecular inhibition of the SH2 and N-terminal domains of STAT3. The strong H-bond interactions between N-terminal, SH2 domain and ligand show that the synthesized compounds are non-selective between STAT3 domain; instead, a strong interaction between ARG-154 and the triazole fragment is observed which can probably be associated to cytotoxic activity in these molecules. The simplicity of synthetic methods and anticancer activities found in some compounds suggests that this class of 4-(1,2,3-triazol-1-yl) salicylic acid derivatives will enjoy a widespread application.

Declaration of Competing Interest

The authors declare that they have no known competing financial interests or personal relationships that could have appeared to influence the work reported in this paper.

CRediT authorship contribution statement

Zita G. Ríos-Malváez: Methodology, Investigation. **Ma-Angeles Cano-Herrera:** Methodology, Investigation. **Juan Carlos Dávila-Becerril:** Software, Investigation. **Gustavo Mondragón-Solórzano:** Software, Data curation, Writing - original draft, Writing - review & editing. **María Teresa Ramírez-Apan:** Methodology, Formal analysis. **David Morales-Morales:** Writing - original draft, Formal analysis. **Joaquín Barroso-Flores:** Data curation, Investigation. **Jonnathan G. Santillán-Benítez:** Conceptualization. **M.V. Basavanag Unnamatla:** Investigation, Methodology. **Marco Antonio García-Eleno:** Formal analysis, Validation, Data curation. **Nelly González-Rivas:** Methodology, Investigation, Formal analysis, Validation. **Erick Cuevas-Yañez:** Conceptualization, Supervision, Project administration, Funding acquisition, Writing - original draft, Writing - review & editing.

Acknowledgments

Financial support from CONACYT (project No. A1-S-18230 and fellowships for ZGRM, CVU: 860116, and GMS, CVU: 771371) is gratefully acknowledged. The authors would like to thank N. Zavala, A. Nuñez, L. Triana and M. C. Martínez for the technical support. JCDB, GMS and JBF want to thank to Dr. Jacinto Sandoval for the academic assessment into the geometry optimizations.

Supplementary materials

Supplementary material associated with this article can be found, in the online version, at doi:10.1016/j.molstruc.2020.129149.

References

[1] D.P. Ball, A.M. Lewis, D. Williams, D. Resetca, D.J. Wilson, P.T. Gunning, Signal transducer and activator of transcription 3 (STAT3) inhibitor, S3I-201, acts as a potent and non-selective alkylating agent, Oncotarget 7 (2016) 20669.
[2] R. Fagard, V. Metelev, I. Souissi, F. Baran-Marszak, STAT3 inhibitors for cancer therapy, JAK-STAT 2 (2013) e22882.
[3] K. Matsuno, Y. Masuda, Y. Uehara, H. Sato, A. Muroya, O. Takahashi, T. Yokotagawa, T. Furuya, T. Okawara, M. Otsuka, N. Ogo, T. Ashizawa, C. Oshita, S. Tai, H. Ishii, Y. Akiyama, A. Asai, Identification of a New Series of STAT3 Inhibitors by Virtual Screening, ACS Med. Chem. Lett. 1 (2010) 371–375.
[4] D. Bhasin, K. Cisek, T. Pandharkar, N. Regan, C. Li, B. Pandit, J. Lin, P.K. Li., Design, synthesis, and studies of small molecule STAT3 inhibitors, Bioorg. Med. Chem. Lett. 18 (2008) 391–395.
[5] C.H. Teng, S.J. Won, C.H. Lin, Design, synthesis and cytotoxic effect of hydroxy and 3-alkylaminopropoxy-9,10-anthraquinone derivatives, Bioorg. Med. Chem. 13 (2005) 3439–3445.
[6] J.A. Drewry, S. Fletcher, P. Yue, D. Marushchak, W. Zhao, S. Sharmeen, X. Zhang, A.D. Schimmer, C. Gradinaru, J. Turkson, PT. Gunning, Coordination complex SH2 domain proteomimetics: an alternative approach to disrupting oncogenic protein–protein interactions, Chem. Commun. 46 (2010) (2010) 892–894.
[7] B.D.G. Page, D.C. Croucher, Z. Li, Y.L. Wong, S. Haftchenary, V.H. Jimenez-Zepeda, J. Atkinson, P.A. Spagnuolo, R. Colagouri, A.M. Lewis, A.D. Schimmer, S. Trudel, P.T. Gunning, Inhibiting Aberrant Signal Transducer and Activator of Transcription (STAT) Protein Activation with Tetrapodal, Small Molecule Src Homology 2 domain binders: Promising Agents Against Multiple Myeloma, J. Med. Chem. 56 (2013) 7190–7200.
[8] S. Fletcher, B.D.G. Page, X. Zhang, P. Yue, Z.H. Li, S. Sharmeen, J. Singh, W. Zhao, A.D. Schimmer, S. Trudel, J. Turkson, P.T. Gunning, Antagonism of the Stat3–Stat3 Protein Dimer with Salicylic Acid Based Small Molecules, ChemMedChem 6 (2011) 1459–1470.
[9] S. Fletcher, J. Singh, X. Zhang, P. Yue, B.D.G. Page, S. Sharmeen, V.M. Shahani, W. Zhao, A.D. Schimmer, J. Turkson, P.t. Gunning, Disruption of Transcriptionally Active Stat3 Dimers with Nonphosphorylated, Salicylic Acid-Based Small Molecules: Potent *in vitro* and Tumor Cell Activities, ChemBioChem 10 (2009) 1959–1964.

[10] E. Bonandi, M.S. Christodoulou, G. Fumagalli, D. Perdicchia, G. Rastelli, D. Passarella, The 1,2,3-triazole ring as a bioisostere in medicinal chemistry, Drug Discov. Today 22 (2017) 1572–1581.

[11] P. Thirumurugan, D. Matosiuk, K. Jozwiak, Click chemistry for drug development and diverse chemical–biology applications, Chem. Rev. 113 (2013) 4905–4979.

[12] S. Haider, M.S. Alam, H. Hamid, 1,2,3-Triazoles: scaffold with medicinal significance, Inflammation Cell Signal. 1 (2014) e95.

[13] S.G. Agalave, S.R. Maujan, V.S. Pore, Click Chemistry: 1,2,3-Triazoles as Pharmacophores, Chem. Asian J. 6 (2011) 2696–2718.

[14] G. Dupuis, An asymmetrical disulfide-containing photoreactive heterobifunctional reagent designed to introduce radioactive labeling into biological receptors, Can. J. Chem. 65 (1987) 2450–2453.

[15] A. Monks, D. Scudiero, P. Skehan, R. Shoemaker, K. Paul, D. Vistica, C. Hose, J. Langley, P. Cronise, A. Vaigro-Wolff, M. Gray-Goodrich, H. Campbell, J. Mayo, M. Boyd, Feasibility of a High-Flux Anticancer Drug Screen Using a Diverse Panel of Cultured Human Tumor Cell Lines, J. Natl. Cancer I. 83 (1991) 757–766.

[16] G.M.J. Frisch, W. Trucks, H.B. Schlegel, G.E. Scuseria, M.A. Robb, J.R. Cheeseman, G. Scalmani, V. Barone, B. Mennucci, G.A. Petersson, H. Nakatsuji, M. Caricato, X. Li, H.P. Hratchian, A.F. Izmaylov, J. Bloino, G. Zheng, J.L. Sonnenberg, Gaussian 09, Revision E.01, Gaussian, Inc., Wallingford, CT, 2009.

[17] N. El-Hachem, B. Haibe-Kains, A. Khalil, F.H. Kobeissy, G. Nemer, in: AutoDock and AutoDockTools for protein-ligand docking: Beta-site amyloid precursor protein cleaving enzyme 1(BACE1) as a case study, in Neuroproteomics. Methods in Molecular Biology, vol. 1598, Humana Press, New York, NY, 2017, pp. pp.391–pp.403.

[18] J.M. Solano-Altamirano, J.M. Hernández-Pérez, DensToolKit: A comprehensive open-source package for analyzing the electron density and its derivative scalar and vector fields, Comput. Phys. Commun. 196 (2015) 362–371.

[19] R. López-González, J. Bautista-Renedo, D. Martínez-Otero, H. Reyes, N. González-Rivas, E. Cuevas-Yañez, 1,4- and 1,5-di(N-phthalimidomethyl)-1,2,3-triazoles: crystal structures and density functional theory studies of the alkyne and azide precursors, J. Chem. Res. 40 (2016) 308–313.

[20] M.J.M. Takac, D.V. Topic, FT-IR and NMR spectroscopic studies of salicylic acid derivatives. II. Comparison of 2-hydroxy- and 2,4- and 2,5-dihydroxy derivatives, Acta Pharm 54 (2004) 177–191.

[21] M.K. Trivedi, A. Branton, D. Trivedi, H. Shettigar, K. Bairwa, S. Jana, Fourier Transform Infrared and Ultraviolet-Visible Spectroscopic Characterization of Biofield Treated Salicylic Acid and Sparfloxacin, Nat. Prod. Chem. Res. 3 (2015) 1000186.

[22] S. Suresh, S. Gunasekaran, S. Srinivasan, Spectroscopic (FT-IR, FT-Raman, NMR and UV–Visible) and quantum chemical studies of molecular geometry, Frontier molecular orbital, NLO, NBO and thermodynamic properties of salicylic acid, Spectrochim. Acta Part A 132 (2014) 130–141.

[23] M. Bellagamba, L. Bencivenni, L. Gontrani, L. Guidoni, C. Sadun, Tautomerism in liquid 1,2,3-triazole: a combined Energy-Dispersive X-Ray Diffraction, Molecular Dynamics and FTIR study, Struct. Chem 24 (2013) 933–943.

[24] F. Billesa, H. Endredi, Keresztury. Vibrational spectroscopy of triazoles and tetrazole, THEOCHEM 530 (2000) 183–200.

[25] S.T. Abu-Orabi, M.A. Atfah, I. Jibril, F.M. Marii, A.A.S. Ali, Dipolar Cycloaddition Reactions of Organic Azides with some Acetylenic Compounds, J. Heterocycl. Chem. 26 (1989) 1461–1468.

[26] C.N.R. Rao, R. Venkataraghavan, Contribution to the Infrared Spectra of Five-Membered N- and N,S-Heterocyclic Compounds, Can. J. Chem. 42 (1964) 43–49.

[27] E. Lieber, C.N.R. Rao, T.S. Chao, H. Rubinstein, The Ultraviolet and Infrared Spectra of Vicinal-Triazole Derivatives, Chem 36 (1958) 1441–1443.

[28] J.A.C. Allison, H.S. El-Khadem, C.A. Wilson, Chloropalladation of 2-phenyl-1,2,3-triazoles as a means of selective o-chlorination, J. Heterocycl. Chem. 12 (1975) 1275–1277.

[29] Y. Tanaka, S.R. Velen, S.I. Miller, Syntheses and Properties of H-1,2,3-Triazoles, Tetrahedron 29 (1973) 3271–3283.

[30] S.I. Miller, R.R. Lii, Y. Tanaka, Mass Spectra of 1,2,3-Triazoles, J. Chem. Soc., Perkin Trans. 1 (1979) 15–19.

[31] A. Maquestiau, Y. Van Haverbeke, M. Willame, M. Begtrup, Fragmentation des 4- et 5-hydroxy -1,2,3-triazoles sous l'impact electronique, Bull. Soc. Chim. Belg. 85 (1976) 795–800.

[32] C. Atef, M. Boualem, M.M. Cherif, H. Youcef, C. Azzedine, Chemical composition and antimicrobial activity of essential oils in Xerophytic plant Cotula cinerea Del (Asteraceae) during two stages of development: flowering and fruiting, J. Appl. Pharm. Sci. 5 (2015) 29–34.

[33] A. Marchese, C.E. Arciola, R. Barbieri, A. Sanches Silva, S.F. Nabavi, A.J.T. Sokeng, M. Izadi, N.J. Jafari, I. Suntar, M. Daglia, S.M. Nabavi, Update on monoterpenes as antimicrobial agents: a particular focus on p-Cymene, Materials 10 (2017) 947.

[34] S.N.J. Moreno, R. Docampo, Mechanism of toxicity of nitro compounds used in the chemotherapy of trichomoniasis, Environ. Health Persp. 64 (1985) 199–208.

[35] T.J. Maimone, P.S. Baran, Modern synthetic efforts toward biologically active terpenes., Nat. Chem. Biol 3 (2007) 396–407.

[36] C. Thirsk, A. Whiting, Polyene natural products, J. Chem. Soc., Perkin Trans. 1 (2002) 999–1023.

[37] R. Kaur, V. Rani, V. Abbot, Y. Kapoor, D. Konar, K. Kumar, Recent synthetic and medicinal perspectives of pyrroles: An overview, J. Pharm. Chem. Chem. Sci. 1 (2017) 17–32.

[38] I.I. Sahay, P.S. Ghalsasi, Synthesis of New 1,2,3-triazole Linked Benzimidazole Molecules as Anti-Proliferative Agents, Synth. Commun. 47 (2017) 825–834.

[39] N. Pokhodylo, O. Shyyka, V. Matiychuk, Synthesis of 1,2,3-Triazole Derivatives and Evaluation of their Anticancer Activity, Sci. Pharm. 81 (2013) 663–676.

[40] M.S. Sonego, N.V. Segatto, L. Damé, M. Fronza, C.B. Gomes, T.L. Oliveira, F.K. Seixas, L. Savegnago, K.M. Schachtschneider, D. Alves, T. Collares, 7-Chloroquinoline-1,2,3-triazoyl carboxamides induce cell cycle arrest and apoptosis in human bladder carcinoma cells, Invest. New Drug. 38 (2020) 1020–1030.

[41] T.M. Queiroz, E.V.M. Orozco, V.R. Silva, L.S. Santos, M.B.P. Soares, D.P. Bezerra, A.L.M. Porto, Semi-synthesis of β-keto-1,2,3-triazole derivatives from ethinylestradiol and evaluation of the cytotoxic activity, Heliyon 5 (2019) e02408.

[42] P. de Andrade, A.F. Dias, F. Figueiro, F.C. Torres, D.F. Kawano, A.M.O. Battastini, I. Carvalho, C.H.T.P. da Silva, J.M. Campos, 1,2,3-Triazole tethered 2-mercaptobenzimidazole derivatives: design, synthesis and molecular assessment toward C6 glioma cell line, Future Med. Chem. 12 (2020) 689–708.

[43] I.C. Chipoline, E. Alves, P. Branco, L.V. Costalotufo, V.F. Ferreira, F.C. Da Silva, Synthesis and Cytotoxic Evaluation of 1H-1,2,3-Triazol-1-ylmethyl-2,3-dihydronaphtho[1,2-b]furan-4,5-diones, Anais da Academia Brasileira de Ciências 90 (1 Suppl. 2) (2018) 1027–1033.

[44] I.C. Chipoline, A.C.C. da Fonseca, G.R.M. da Costa, M.P. de Souza, V.W.H. Rabelo, L.N. de Queiroz, T.L.F. de Souza, E.C.P. de Almeida, P.A. Abreu, B. Pontes, V.F. Ferreira, F.C. da Silva, B.K. Robbs, Molecular mechanism of action of new 1,4-naphthoquinones tethered to 1,2,3-1h-triazoles with cytotoxic and selective effect against oral squamous cell carcinoma, Bioorg. Chem. 101 (2020) 103984.

[45] Y. Jia, M. Li, Y. Cao, W. Feng, X. Li, W. Xue, H. Shi, Discovery of a Novel Benzenesulfonamide Analogue That Inhibits Proliferation and Metastasis Against Ovarian Cancer OVCAR-8 Cells, Drug. Des. Dev. Ther. 14 (2020) 207–216.

[46] Z. Liu, X. Ge, Y. Gu, Y. Huang, H. Liu, M. Yu, Y. Liu, Small molecule STAT3 inhibitor, 6Br-6a suppresses breast cancer growth *in vitro* and *in vivo*., Biomed. Pharmacother. 121 (2020) 109502.

[47] L. Yang, S. Lin, L. X, J. Lin, C. Zhaob, X. Huang, Novel activators and small–molecule inhibitors of STAT3 in cancer, Cytokine Growth Factor Rev. 49 (2019) 10–22.

[48] P. Yue, J. Turkson, Targeting STAT3 in cancer: how successful are we? Expert Opin, Investig. Drugs 18 (2009) 45–56.

[49] Y. Tsujita, A. Horiguchi, S. Tasaki, M. Isono, T. Asano, K. Ito, T. Asano, Y. Mayumi, T. Kushibiki, STAT3 inhibition by WP1066 suppresses the growth and invasiveness of bladder cancer cells, Oncol. Rep. 38 (2017) 2197–2204.

[50] F. Barbieri, S. Thellung, A. Ratto, E. Carra, V. Marini, C. Fucile, A. Bajetto, A. Pattarozzi, R. Würth, M. Gatti, C. Campanella, G. Vito, F. Mattioli, A. Pagano, A. Daga, A. Ferrari, T. Florio, *In vitro* and in vivo antiproliferative activity of metformin on stem-like cells isolated from spontaneous canine mammary carcinomas: translational implications for human tumors, BMC Cancer 15 (2015) 228.

[51] C.A. Riedl, L.S. Flocke, M. Hejl, A. Roller, M.H.M. Klose, M.A. Jakupec, W. Kandioller, B.K. Keppler, Introducing the 4-Phenyl-1,2,3-Triazole Moiety as a Versatile Scaffold for the Development of Cytotoxic Ruthenium(II) and Osmium(II) Arene Cyclometalates, Inorg. Chem. 56 (2017) 528–541.

[52] F.S. Zariquiey, J.V. Da Souza, R. Estrada-Tejedor, A.K. Bronowska, If you cannot win them, join them: understanding new ways to target stat3 by small molecules, ACS Omega 4 (2019) 13913–13921.

[53] M.A. Al Noman, T. Hossain, M. Ahsan, S. Jamshidi, C.M. Hasan, K.M. Rahman, Crispenes F and G, cis-Clerodane Furanoditerpenoids from Tinospora crispa, Inhibit STAT3 Dimerization, J. Nat. Prod. 81 (2018) 236–242.

[54] T. Ashizawa, A. Iizuka, C. Maeda, E. Tanaka, R. Kondou, H. Miyata, T. Sugino, T. Kawata, S. Deguchi, K. Mitsuya, N. Hayashi, A. Asai, M. Ito, K. Yamaguchi, Y. Akiyama, Impact of combination therapy with anti-PD-1 blockade and a STAT3 inhibitor on the tumor-infiltrating lymphocyte status, Immunol. Lett. 216 (2019) 43–50.